AMERICAN SOCIETY FOR MICROBIOLOGY | Infection and Immunity®

BACTERIAL INFECTIONS

Protein Acetylation Mediated by YfiQ and CobB Is Involved in the Virulence and Stress Response of *Yersinia pestis*

Wanbing Liu,[a] Yafang Tan,[a] Shiyang Cao,[a] Haihong Zhao,[b] Haihong Fang,[a] Xiaoyan Yang,[b] Tong Wang,[a] Yazhou Zhou,[a] Yanfeng Yan,[a] Yanping Han,[a] Yajun Song,[a] Yujing Bi,[a] Xiaoyi Wang,[a] Ruifu Yang,[a] Zongmin Du[a]

[a]State Key Laboratory of Pathogen and Biosecurity, Beijing Institute of Microbiology and Epidemiology, Beijing, China

[b]Key Laboratory for Plague Prevention and Control of Qinghai Province 2017-ZJ-Y15, Institute for Endemic Disease Prevention and Control of Qinghai Province, Xining, China

ABSTRACT Recent studies revealed that acetylation is a widely used protein modification in prokaryotic organisms. The major protein acetylation acetyltransferase YfiQ and the sirtuin-like deacetylase CobB have been found to be involved in basic physiological processes, such as primary metabolism, chemotaxis, and stress responses, in *Escherichia coli* and *Salmonella*. However, little is known about protein acetylation modifications in *Yersinia pestis*, a lethal pathogen responsible for millions of human deaths in three worldwide pandemics. Here we found that *Yp_0659* and *Yp_1760* of *Y. pestis* encode the major protein acetylation acetyltransferase YfiQ and the sirtuin-like deacetylase CobB, respectively, which can acetylate and deacetylate PhoP enzymatically *in vitro*. Protein acetylation impairment in *cobB* and *yfiQ* mutants greatly decreased bacterial tolerance to cold, hot, high-salt, and acidic environments. Our comparative transcriptomic data revealed that the strongly decreased tolerance to stress stimuli was probably related to downregulation of the genes encoding the heat shock proteins (HtpG, HslV, HslR, and IbpA), cold shock proteins (CspC and CspA1), and acid resistance proteins (HdeB and AdiA). We found that the reversible acetylation mediated by CobB and YfiQ conferred attenuation of virulence, probably partially due to the decreased expression of the *psaABCDEF* operon, which encodes Psa fimbriae that play a key role in virulence of *Y. pestis*. This is the first report, to our knowledge, on the roles of protein acetylation modification in stress responses, biofilm formation, and virulence of *Y. pestis*.

KEYWORDS *Yersinia pestis*, pathogenesis, protein acetylation, stress response

N^{ε}-lysine acetylation was first identified in the 1960s as a reversible and highly regulated posttranslational modification, and at that time it was thought to occur only in eukaryotic cells (1). In eukaryotic cells, protein acetylation is mainly linked to transcriptional regulation. Acetylated histones increase their negative charge and decrease their interactions with DNA, which leads to a lower nucleosome compactness and makes the DNA accessible to the proteins required to initiate transcription and activate downstream gene transcription (2). With advances in mass spectrometry (MS)-based proteomics and high-affinity purification of acetylated peptides, more and more studies have revealed that acetylated proteins are present in various types of bacteria, indicating that protein acetylation is a common phenomenon that occurs widely across all the domains of life. Acetylated proteins have been identified by use of proteomics on various bacteria, such as *Escherichia coli*, *Bacillus subtilis*, *Salmonella* spp., and *Mycobacterium tuberculosis* (3–7), and more and more acetylated proteins and acetylation sites have been identified in the model organism *E. coli* by different groups in recent years. Castano-Cerezo identified 809 acetylated proteins and more than 2,000 acetylated sites in *E. coli* (8). Functional studies of these acetylated proteins revealed

Received 27 March 2018 **Accepted** 28 March 2018

Accepted manuscript posted online 2 April 2018

Citation Liu W, Tan Y, Cao S, Zhao H, Fang H, Yang X, Wang T, Zhou Y, Yan Y, Han Y, Song Y, Bi Y, Wang X, Yang R, Du Z. 2018. Protein acetylation mediated by YfiQ and CobB is involved in the virulence and stress response of *Yersinia pestis*. Infect Immun 86:e00224-18. https://doi.org/10.1128/IAI.00224-18.

Editor Manuela Raffatellu, University of California San Diego School of Medicine

Address correspondence to Ruifu Yang, ruifuyang@gmail.com, or Zongmin Du, zmduams@163.com.

W.L. and Y.T. contributed equally to this article.

TABLE 1 Comparative sequence analysis of *cobB* and *yfiQ* (also called *pat*) orthologous homologs in *Y. pestis*, *E. coli*, and *S. enterica*

	Y. pestis 91001		*E. coli* K-12 MG1655			*S.* Typhimurium LT2		
Function	Gene	Length (bp)	Gene	Length (bp)	Identity (%)	Gene	Length (bp)	Identity (%)
Protein deacetylase	*Yp_1760*	837	*cobB* (NAD^+-dependent sirtuin gene)	729	70.4	*cobB* (NAD^+-dependent sirtuin gene)	831	68.5
Protein acetyltransferase	*Yp_0659*	2,643	*yfiQ*	2,661	70.4	*pat*	2,674	68.8

that they are mainly associated with carbon source metabolism, transcriptional regulation, and protein stability. Among the different bacterial species, most of these acetylated proteins share homology, indicating that acetylation is an evolutionarily conserved protein modification (6, 7).

YfiQ (Pat in *Salmonella enterica*), a Gnc-5-like acetyltransferase, catalyzes the transfer of an acetyl group from acetyl-coenzyme A (Ac-CoA) to its substrate (9). In *M. tuberculosis*, the lysine acetyltransferase is regulated by cAMP, a major virulence factor in this pathogen (10). CobB, an NAD^+-dependent (Sir2-like) deacetylase, was heretofore the only known deacetylase in *E. coli* (8). In recent years, the physiological implications of lysine acetylation in prokaryotes have been studied intensively. Acetyl-CoA synthetase (Acs) was the first enzyme to be described as being reversibly regulated by lysine acetylation. This enzyme is inactivated upon acetylation of a single active-site lysine residue (Lys609) by Pat (11), and acetylated Acs is then reactivated by NAD^+-dependent deacetylation by the CobB deacetylase (12). Many biological components or enzymes (e.g., the CheY chemotaxis response regulator, RNA polymerase, the capsule synthesis regulator [RcsB], RNase R, and *N*-hydroxyarylamine *O*-acetyltransferase) are subject to protein acetylation (13–19).

Despite recent progress, little is known about protein acetylation in bacteria other than *E. coli* and *S. enterica*, and no protein acetylation system has been characterized for the causative agent of plague, *Yersinia pestis*, which has been responsible for three worldwide pandemics in human history. Plague is a zoonotic disease transmitted by flea vectors, and rodents are the main reservoir host, whereas humans are only accidental hosts. During transmission to and infection of the mammalian host, *Y. pestis* is subjected to various environmental challenges, such as temperature variations, acidic pH, and oxidative stress, among others (2). To survive in adverse environments, *Y. pestis* must rapidly adapt to various stimuli. It achieves this via multiple regulatory mechanisms (transcriptional, translational, and posttranslational) that are mediated by different posttranslational modifications, including protein acetylation.

In the present study, we investigated how protein acetylation modifications affect the physiology of *Y. pestis*. First, we constructed null mutants of the YfiQ major acetyltransferase and CobB deacetylase in *Y. pestis* strain 201, and we found that the two mutants showed defects in responses to different stress stimuli, such as hot, cold, acidic, and high-salt environments. We found that biofilm formation and pathogenesis were regulated by protein acetylation and that both the Δ*cobB* and Δ*yfiQ* strains exhibited attenuated virulence and biofilm formation.

RESULTS

Identification of major acetyltransferase and deacetylase in *Y. pestis*. According to the genome annotation of *Y. pestis* strain 91001, *YP_1760* encodes a putative Sir2 family protein and *YP_0659* a putative acetyltransferase (20, 21). Sequence alignments indicate that *YP_1760* shares high similarity with *cobB* from the model bacteria *E. coli* K-12 (70.4%) and *S. enterica* (68.5%) (Table 1). *YP_0659* is highly similar to *yfiQ* (or *pat*) of *E. coli* K-12 and *S. enterica*, with 70.4% and 68.8% sequence identities, respectively (Table 1). Quantitative reverse transcription-PCR (qRT-PCR) analysis showed that expression of *YP_0659* is relatively low during the exponential phase but is upregulated upon reaching the stationary phase, whereas expression of *YP_1760* appears to be independent of the growth stage (see Fig. S1 in the supplemental material). These

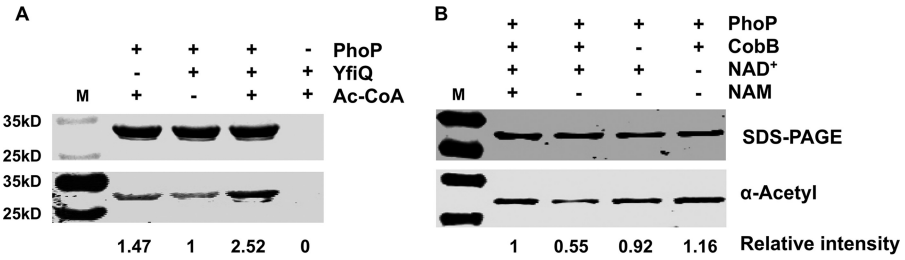

FIG 1 PhoP can be acetylated by *Y. pestis* YfiQ and deacetylated by CobB *in vitro*. (A) YfiQ acetylates PhoP *in vitro*. Purified recombinant PhoP (0.2 μg/μl) was incubated with or without YfiQ (0.1 μg/μl) and Ac-CoA (0.2 mM) in acetylation reaction buffer. (B) CobB deacetylates PhoP *in vitro*. Purified PhoP (0.2 μg/μl) was incubated with or without CobB (0.1 μg/μl), NAM (40 mM), and NAD^+ (4 mM) in deacetylation reaction buffer. The acetylation levels were determined by immunoblotting, and the results shown here are representative of at least three independent replicates. Band intensities were quantitated using ImageJ software. M, molecular size marker.

features are consistent with the expression characters of *cobB* and *yfiQ* in *E. coli* K-12 (14). The upregulated expression of *yfiQ* in the stationary phase is consistent with the previous finding that acetylated proteins are more abundant in the stationary phase (3). Sequence alignment analysis of the *cobB* and *yfiQ* genes by BLAST searches at the NCBI website found that both genes share 100% identity among the 39 *Y. pestis* strains that have been sequenced completely, indicating that both the *cobB* and *yfiQ* genes are highly conserved in *Y. pestis* and that characterization of their functions in this study would be applicable to other *Y. pestis* strains.

Collectively, these data indicate that *YP_1760* and *YP_0659* in *Y. pestis* encode homologs of the CobB and YfiQ proteins of *Salmonella*, respectively. Thus, we designated the *YP_1760* and *YP_0659* genes *cobB* and *yfiQ*, respectively, for *Y. pestis* strain 201.

PhoP can be reversibly acetylated *in vitro* by YfiQ and CobB. It has been reported that the two-component regulatory protein PhoP can be acetylated by YfiQ and deacetylated by CobB in *S. enterica* serovar Typhimurium (22). Therefore, to investigate whether the same phenomenon occurs in *Y. pestis*, we cloned the *yfiQ* coding sequence into pGEX-4T-2 and the *cobB* and *phoP* coding sequences into pET-28a, expressed the recombinant proteins in *E. coli* BL21, and then purified them. *In vitro* assays involving acetylation of PhoP by YfiQ and deacetylation of PhoP by CobB in *Y. pestis* strain 201 were performed. Our results showed that purified YfiQ exhibits an acetylation activity toward PhoP *in vitro*, in an Ac-CoA-dependent manner (Fig. 1A). Additionally, the CobB deacetylation activity toward PhoP is NAD^+ dependent and is inhibited by the presence of nicotinamide (NAM), a Sir2 inhibitor (Fig. 1B).

Construction of *cobB* and *yfiQ* mutants and complemented strains. To investigate how protein acetylation affects the physiology of *Y. pestis*, *cobB* and *yfiQ* mutants of *Y. pestis* strain 201 were constructed using the λ Red-based recombination strategy, and the corresponding complemented strains (Table 2) were constructed as described in Materials and Methods. Immunoblots were used to detect the expression of CobB and YfiQ, and the results confirmed that the mutants and complemented strains had been constructed successfully (Fig. 2). Growth comparisons were made for the wild-type bacterium and the *Y. pestis* mutants in Luria-Bertani (LB) broth and TMH medium (23), and neither mutant (*cobB* or *yfiQ*) showed a significant difference in growth rate from that of the wild-type strain (Fig. S2), indicating that the loss of *cobB* or *yfiQ* showed limited effects on the growth of the mutant strains. Therefore, our phenotypic analysis of the *cobB* and *yfiQ* mutants in comparison with the wild-type strain should not be affected by growth rate differences.

Comparative transcriptomic analysis of wild-type *Y. pestis* against the *cobB* and *yfiQ* mutants. To gain functional insight into the protein acetylation modification mediated by YfiQ and CobB in *Y. pestis*, we compared the transcriptional profiles of the *cobB* and *yfiQ* mutants to that of the wild-type strain by using RNA sequencing (RNA-seq). Six cDNA libraries were constructed for RNA-seq analysis. Clean reads from

TABLE 2 Strains and plasmids used in this study

Strain or plasmid	Relevant description or characteristics	Source or reference
Strains		
Y. pestis strains		
Y. pestis strain 201	Wild-type *Yersinia pestis* bv. Microtus strain 201	39
Δ*cobB*	*Yersinia pestis cobB* gene knockout	This study
Δ*yfiQ*	*Yersinia pestis yfiQ* gene knockout	This study
Com-*cobB*	Δ*cobB* strain complemented by introduction of plasmid pACYC184-*cobB*	This study
Com-*yfiQ*	Δ*yfiQ* strain complemented by introduction of plasmid pACYC184-*yfiQ*	This study
E. coli strains		
Exp-*cobB*	BL21(DE3) containing plasmid pACYC184-*cobB*, expressing His-CobB	This study
Exp-*yfiQ*	BL21(DE3) containing plasmid pGEX-4T-*yfiQ*, expressing GST-YfiQ	This study
Exp-*phoP*	BL21(DE3) expressing His-PhoP protein	Laboratory collection
Plasmids		
pACYC184-*cobB*	*cobB* coding sequence and 426 bp of upstream sequence cloned into SphI/SalI sites of pACYC184; Cm^r	This study
pACYC184-*yfiQ*	*yfiQ* coding sequence and 426 bp of upstream sequence cloned into BamHI/SalI sites of pACYC184; Cm^r	This study
pET28a-*cobB*	*cobB* gene inserted into pET28a; Km^r	This study
pGEX-4T-*yfiQ*	*yfiQ* gene inserted into pGEX-4T-2; Ap^r	This study
pKD46	Temperature-sensitive plasmid expressing λ Red recombinase under the control of arabinose; Ap^r	Laboratory collection
pCP20	Temperature-sensitive plasmid expressing FLP recombinase; Ap^r Cm^r	Laboratory collection
pKD4	Template plasmid in the λ Red system for Km^r gene cassette; Km^r	Laboratory collection

the RNA-seq data were mapped to the annotated genome of *Y. pestis* bv. Microtus strain 91001. Each sample yielded about 2.0×10^7 clean reads, and 98% of the reads (on average) were uniquely mapped to the reference genome. Gene expression was quantified as fragments per kilobase of transcript sequence per million fragments mapped (FPKM), and the differences in gene expression among the mutants and the wild-type strain were calculated by use of the R DESeq package (24). The resulting *P* values were adjusted using Benjamini and Hochberg's approach for controlling the false-discovery rate. Genes with an adjusted *P* value of <0.05 and a $|\log_2$ fold change$|$ value of ≥ 1 were considered to be differentially expressed genes (DEGs).

We found 399 DEGs in the *cobB* mutant, among which 142 were downregulated and 257 were upregulated in comparison to the levels in the wild-type strain (Fig. 3A). DEGs were classified according to their functional categories, and the most significantly affected gene categories were cell envelope and transcription/binding proteins, followed by chemotaxis and mobility, regulatory function, and metabolism (Fig. S3A).

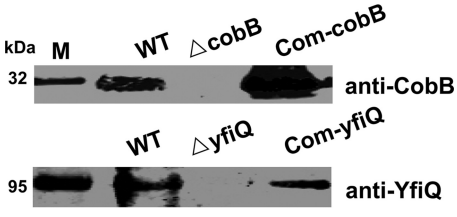

FIG 2 Immunoblot detection of CobB and YfiQ expression in the *Y. pestis yfiQ* and *cobB* mutants. Expression of CobB and YfiQ in the wild-type strain, the *cobB* and *yfiQ* mutants, and the complemented strains was detected by immunoblotting using rabbit anti-YfiQ and -CobB antibodies and an IRDye 800CW-conjugated goat anti-rabbit secondary antibody.

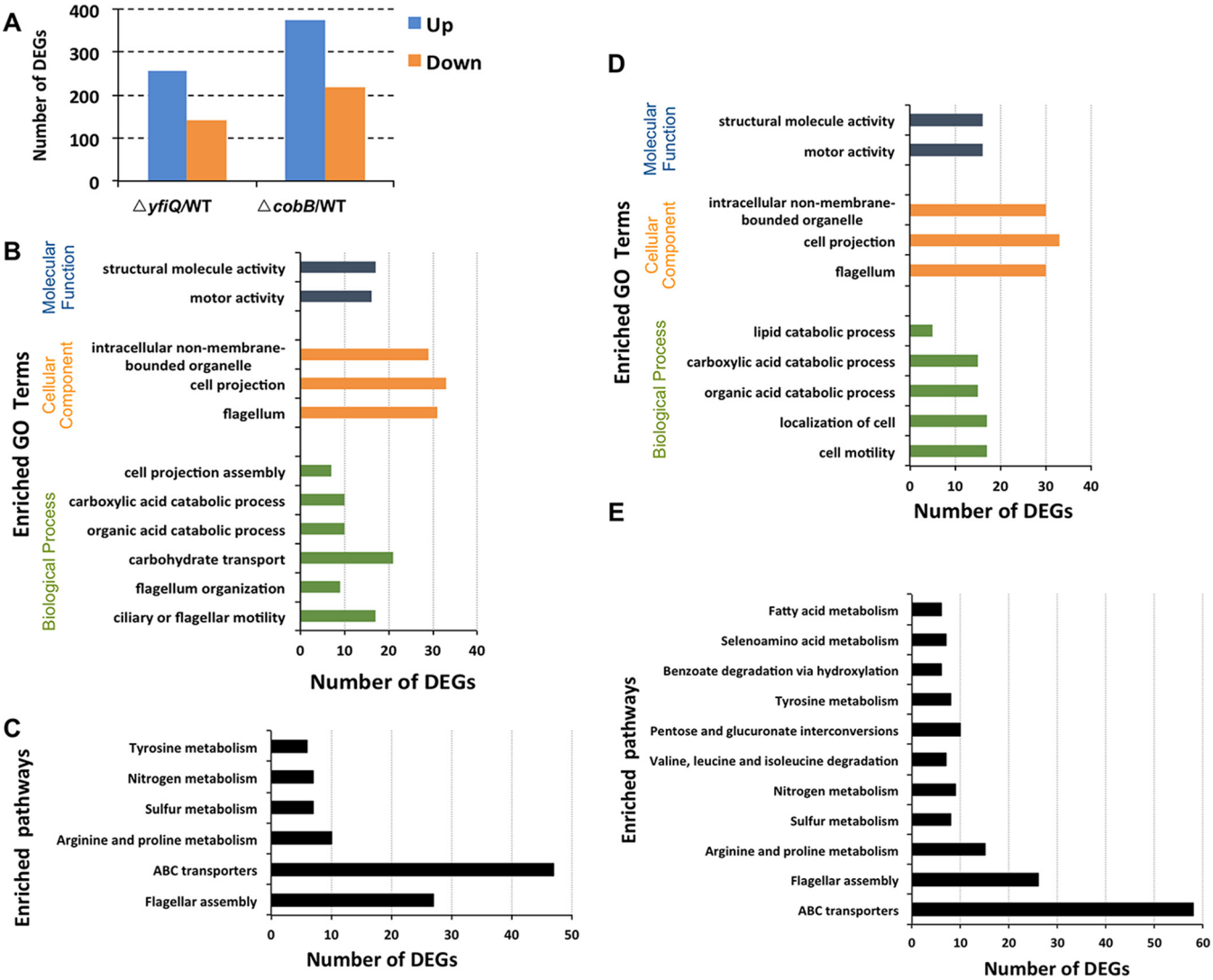

FIG 3 Comparative transcriptome analysis of the wild-type strain and the *cobB* and *yfiQ* mutants of *Y. pestis*. (A) Numbers of DEGs that were significantly differentially expressed in the *cobB* and *yfiQ* mutants in comparison to the wild-type strain, according to the RNA-seq results. The enrichment analysis of DEGs in the mutants was performed using DAVID bioinformatics tools. The GO terms and KEGG pathways enriched significantly in the *cobB* (B and C) and *yfiQ* (D and E) mutants are shown.

Functional enrichment analysis of DEGs was performed using DAVID bioinformatics tools (25) and according to the Kyoto Encyclopedia of Genes and Genomes (http://www.genome.jp/kegg/) and Gene Ontology (GO) annotations. Pathways or GO terms that were enriched significantly in DEGs ($P < 0.05$ by Fisher's exact test followed by the Benjamini multiple-testing correction) are shown in Fig. 3B and C. Cellular functions associated with chemotaxis, flagellar assembly, and metabolism were significantly affected when the *cobB* gene was deleted, which is consistent with previous reports (4, 8, 15). Although *Y. pestis* is nonmotile due to a frameshift mutation in *flhD*, the regulatory role of acetylation modification in chemotaxis can still be observed. There were 594 DEGs in the *yfiQ* mutant, among which 219 were downregulated and 375 were upregulated in comparison to the levels in the wild-type strain (Fig. 3A). Functional analysis of DEGs again found that cellular functions associated with flagellar assembly and metabolism were significantly expressed in the *yfiQ* mutant (Fig. 3D and E; Fig. S3B). Interestingly, our data revealed that ABC transporters were significantly altered in both the *cobB* and *yfiQ* mutants, indicating that the exchanges of substances between the bacterial cells and the outside environments were substantially influenced

TABLE 3 Stress response- and virulence-related genes that were differentially expressed between the mutants and wild-type *Y. pestis*

Gene ID	Gene name	Gene product	Log_2 ratio of fold changes	
			Δ*cobB*/WT	Δ*yfiQ*/WT
Virulence genes				
YP_1290	*psaF*	Hypothetical protein	−4.34	−4.14
YP_1289	*psaA*	Adhesin	−2.62	−2.07
YP_1291	*psaE*	Regulatory protein	−3.78	−4.15
YP_1288	*psaB*	Chaperone protein PsaB	−2.10	−4.07
YP_1698	*hmsS*	Hemin storage system protein	−2.14	−1.94
YP_1697	*hmsR*	*N*-Glycosyltransferase	−1.82	−1.94
YP_1695	*hmsH*	Hypothetical protein	−1.11	−1.81
YP_1696	*hmsF*	Outer membrane *N*-deacetylase	−1.54	−2.09
YP_1764	*phoP*	DNA-binding transcriptional regulator PhoP	0.87	1.23
YP_0141	*hslR*	Heat shock protein 15	−0.57	−1.01
YP_2160	*slyA*	MarR family transcriptional regulatory protein	−2.11	−2.19
YP_pPCP08	*pla*	Outer membrane protease	1.04	1.43
YP_0910	*pla2*	Outer membrane protease	4.00	3.52
Stress response genes				
YP_2475	*hdeB*	Acid resistance protein	−1.54	−0.99
YP_0936	*adiA*	Amino acid decarboxylase	−4.00	−3.77
YP_1228	*cspD*	Cold shock-like protein	1.26	1.49
YP_3903	*cspa1*	Major cold shock protein Cspa1	−0.57	−1.23
YP_1764	*phoP*	DNA-binding transcriptional regulator PhoP	0.87	1.23
YP_0811	*htpG*	Heat shock protein 90	−1.15	−0.84
YP_0108	*hslV*	Heat shock protein	−1.05	−1.01
YP_0141	*hslR*	Heat shock protein 15	−0.57	−1.01
YP_3994	*ibpA*	Heat shock protein IbpA	−1.14	−0.35
YP_0397	*lytT*	Two-component response-regulatory protein YehT	1.00	1.45
YP_3333	*uspA2*	Universal stress protein A	0.89	1.58

in the mutants. Taken together, these results indicate that CobB- and YfiQ-mediated protein acetylation modification has a broad regulatory role in the physiological features of *Y. pestis*.

Interestingly, expression of the virulence-related genes *hmsHFRS* and *psaABCDEF* was significantly lower in both the Δ*cobB* and Δ*yfiQ* mutants (Table 3). Moreover, the stress response-related genes involved in the heat and cold shock responses, acid resistance, and the universal stress response were significantly differentially expressed. Most of these genes, for example, *hdeB*, *adiA*, *htpG*, *hslV*, *hslR*, *ibpA*, and *cspa1*, were significantly downregulated, while a few of them (*cspD*, *phoP*, *lytT*, and *uspA2*) were significantly upregulated (Table 3).

To validate the findings revealed by the RNA-seq analysis, primer pairs for 19 genes (Table S1) involved in virulence or stress responses were designed for qRT-PCR, and the cDNAs reverse transcribed from the RNA samples used for RNA-seq analysis were used as templates for qRT-PCR. Gene transcript levels were normalized to 16S rRNA gene expression, and the log_2 ratios of the expression levels between the wild-type strain and each mutant were calculated for each of the tested genes. Comparative analysis of the results from qRT-PCR and RNA-seq showed that correlation between the two measurements was sufficiently high (Fig. S4; Table S2) to indicate that the RNA-seq data set for this study is highly reliable.

Both *cobB* and *yfiQ* mutants exhibit virulence attenuation in mice. Because a lot of the genes involved in virulence were downregulated in both *cobB* and *yfiQ* mutants, we sought to determine whether the two strains exhibit virulence attenuation in mice. Groups of BALB/c mice ($n = 10$) were infected with the wild type or the *cobB* or *yfiQ* mutant via subcutaneous injections of about 100 CFU. The *cobB* mutant displayed a slight but statistically significant virulence attenuation in mice ($P < 0.05$ by the log rank [Mantel-Cox] test), and the survival time of mice infected with the *cobB* mutant was 7 days, i.e., survival was prolonged by 1 day, on average, compared to the survival of 6 days for mice infected with the wild-type strain (Fig. 4A), whereas the Δ*yfiQ* strain exhibited more significant virulence attenuation ($P < 0.05$ by the log rank [Mantel-Cox]

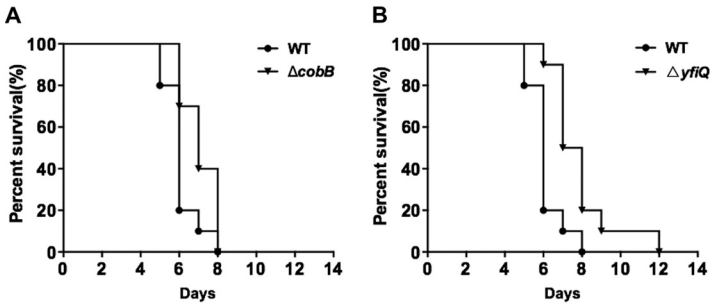

FIG 4 *Y. pestis yfiQ* and *cobB* mutants exhibit virulence attenuation in mice. Groups of BALB/c mice ($n = 10$) were subcutaneously infected with about 100 CFU of the *Y. pestis* wild-type strain or the Δ*cobB* (A) or Δ*yfiQ* (B) strain and then observed continuously for 14 days. The survival curves were plotted against the day postinfection by using GraphPad Prism 5.0, and the significance of differences between the wild-type strain and the mutants was analyzed by the log rank (Mantel-Cox) test (for the wild type versus the *cobB* mutant, $P = 0.03$; for the wild type versus the *yfiQ* mutant, $P = 0.004$).

test) (Fig. 4B). These results show that CobB- and YfiQ-mediated protein acetylation is involved in the virulence of *Y. pestis* and that the differentially expressed virulence-associated genes (Table 3) in the mutants might have contributed to the virulence attenuation.

Protein acetylation modification regulates the cellular stress response in *Y. pestis*. To investigate whether protein acetylation impairment in the *cobB* and *yfiQ* mutants affects the stress response and other physiological functions in *Y. pestis*, tolerance to various stress stimuli was analyzed in the mutants. The *cobB* and *yfiQ* mutants were more sensitive to cold shock than the wild-type strain, irrespective of the treatment temperature (−20, 0, or 4°C) (Fig. 5A). Similarly, when they were treated with heat or acid stress, the *cobB* and *yfiQ* mutants also displayed significantly decreased survival rates (Fig. 5B and C). The growth curves for the mutants grown in high-salt medium (LB broth containing 4% NaCl) were then compared to that for the wild-type strain grown in the same medium. Growth retardation was observed for all the tested strains upon exposure to the high-salt medium compared to the bacterial growth in LB broth containing 1% NaCl; however, the *cobB* and *yfiQ* mutants clearly suffered stronger restriction than the wild-type strain, and tolerance of the high-salt environment was restored to that of the wild type in the complemented strains (Fig. 5D).

Mutation of the major acetyltransferase YfiQ or the deacetylase CobB might lead to acetylation alterations of the *Y. pestis* proteome. Therefore, to investigate whether the acetylated protein profiles in wild-type *Y. pestis* differ from those of the *cobB* and *yfiQ* mutants in response to various stress conditions, the bacterial strains were grown in TMH medium to an approximate optical density at 620 nm (OD_{620}) of 1.0 and then subjected to heat or acid stress. The bacterial cells were harvested after treatment and analyzed by immunoblotting with an anti-acetyl-lysine antibody. Multiple protein bands spanning a wide mass range were detected, and the acetylated protein profiles showed different patterns among the different treatments (Fig. 6A), whereas sodium dodecyl sulfate-polyacrylamide gel electrophoresis (SDS-PAGE) analysis of the same samples resulted in largely similar patterns among the different treatments (Fig. 6B), indicating that heat and acid stress conditions had marked effects on the acetylation proteome of *Y. pestis*. Notably, several bands showed significantly different abundances among the wild-type, Δ*cobB*, and Δ*yfiQ* strains (Fig. 6A), suggesting that YfiQ and CobB may be involved in acetylation modification of those proteins.

Taken together, these results show that the tolerance of the *cobB* and *yfiQ* mutants to stress stimuli, such as cold shock, heat shock, high-salt, and acidic stress conditions, was significantly impaired and that the protein acetylation modification mediated by YfiQ and CobB contributes significantly to the stress response of *Y. pestis*.

Biofilm formation ability is increased in the *cobB* and *yfiQ* mutants. Next, we sought to determine whether biofilm formation by *Y. pestis* is affected by mutations of

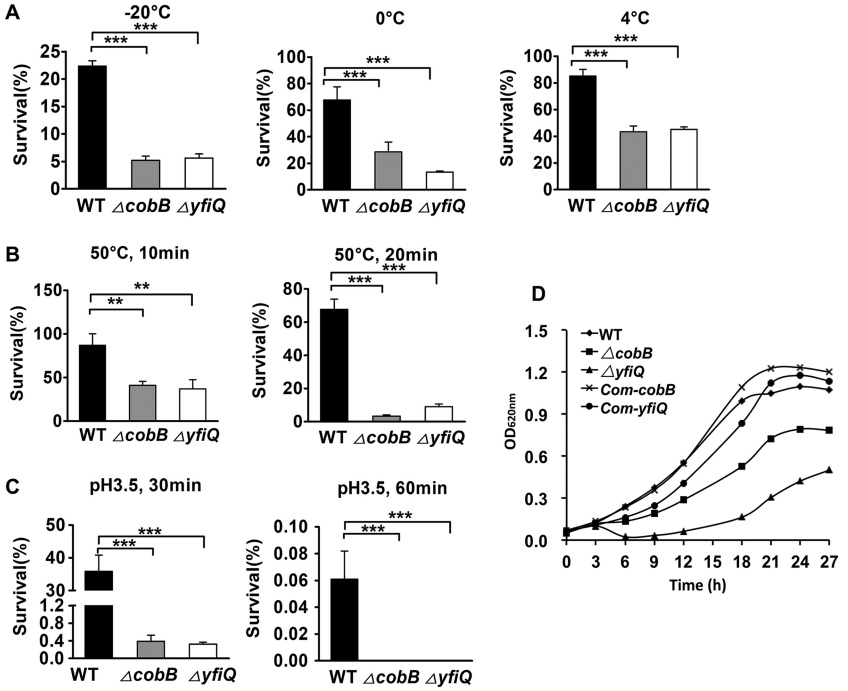

FIG 5 *Y. pestis cobB* and *yfiQ* mutants have lowered resistance to various stress conditions. The survival rates of the wild-type, Δ*cobB*, and Δ*yfiQ* strains after incubation overnight at −20, 0, or 4°C (A), incubation at 50°C for 10 or 20 min (B), or incubation at pH 3.5 for 30 or 60 min (C) were calculated and are shown as the means and SD for three replicates. ANOVA with Dunnett's multiple-comparison test was used to analyze the differences between the treated samples and the controls (***, $P < 0.001$; **, $P < 0.01$). (D) The growth of the Δ*cobB* and Δ*yfiQ* strains was significantly impaired in LB broth containing 4% NaCl compared to that of the wild-type strain, whereas the growth of the complemented strains was restored to that of the wild-type bacterium. Two independent experiments were performed, and results representative of one experiment are shown here.

cobB and *yfiQ* due to the observation that the expression of *hmsHFRS*, which is responsible for the synthesis and translocation of the biofilm matrix, is much lower in both mutants, as revealed by our comparative transcriptomic study. Bacterial strains were inoculated into 24-well plates, and biofilms adhered to the walls of the wells were detected by crystal violet staining (26). Surprisingly, biofilm formation of both the *cobB* and *yfiQ* mutants increased significantly compared to that of the wild-type strain,

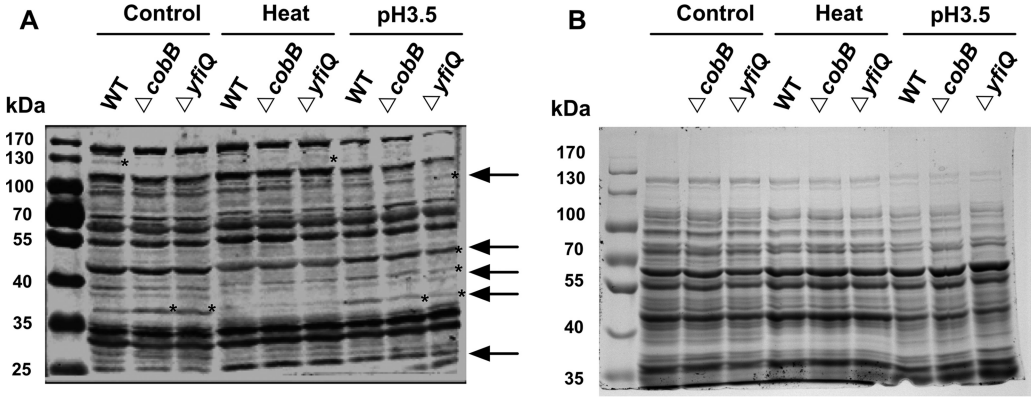

FIG 6 The acetylated protein profiles of the *Y. pestis* strains under various stress conditions showed significant differences. The wild-type, Δ*cobB*, and Δ*yfiQ* strains of *Y. pestis* were incubated at 50°C for 20 min or at pH 3.5 for 30 min as described in Materials and Methods. The bacterial cells were then harvested and analyzed by immunoblotting using an anti-acetyllysine antibody (A) and by SDS-PAGE followed by Coomassie blue staining (B). At least three experiments were performed, from which similar results were obtained, and representative results are shown here. Asterisks denote the protein bands with different abundances among the strains.

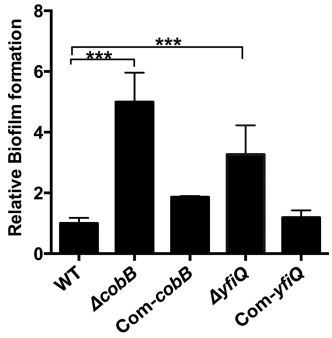

FIG 7 *Y. pestis cobB* and *yfiQ* mutants have an increased ability to form biofilms. *Y. pestis* strains were grown in 24-well polystyrene plates, and the bacterial biomass adhering to the walls of the wells was stained with crystal violet to determine the OD_{570} values. Planktonic cells were used to determine the OD_{620} values. The relative capacity to form biofilms for each strain tested is shown as the OD_{570}/OD_{620} value, followed by normalization using the OD_{570}/OD_{620} value for wild-type *Y. pestis*. ANOVA with Dunnett's multiple-comparison test was used to analyze the differences between the various strains (***, $P < 0.001$).

whereas the mutant strains complemented with the CobB and YfiQ expression plasmids showed a restored, wild-type biofilm formation ability (Fig. 7). We speculate that the key players in biofilm formation other than *hmsHFRS* might also be influenced by the deletion of *cobB* or *yfiQ*, leading to a complex effect on the biofilm formation ability of the mutants. For instance, *Y. pestis* produces HmsT/HmsD diguanylate cyclases to synthesize c-di-GMP, which is required for biofilm formation, and SlyA promotes biofilm formation via directly inhibiting *hmsT* transcription. We found that expression of SlyA decreased >4-fold, which probably contributed to the observed higher levels of biofilm formation of the *cobB* and *yfiQ* mutants. These results demonstrate that protein acetylation modification significantly influences biofilm formation in *Y. pestis* by affecting multiple proteins involved in this process.

DISCUSSION

In the present study, to investigate the role of protein acetylation in various physiological processes, the phenotypes of the *cobB* mutant, the *yfiQ* mutant, and the wild-type *Y. pestis* strain were compared for their responses to adverse environments, biofilm formation abilities, and virulence characteristics.

Our results showed that when the *yfiQ* or *cobB* gene was deleted, no significant growth differences were observed compared to the growth of the wild-type *Y. pestis* strain. Therefore, the phenotypic changes observed in this study were not influenced by any growth differences among the strains. *cobB* expression did not change during the different growth phases, whereas, in common with previous results for *E. coli*, *yfiQ* expression peaked in the stationary phase (14). The observation that *yfiQ* was more highly expressed during the stationary phase coincides with the established finding that acetylated proteins are found in greater abundance in stationary-phase cultures (3). Our comparative transcriptomic study found that the *cobB* and *yfiQ* deletions resulted in differential expression of a large number of genes. Cellular functions associated with chemotaxis, flagellar assembly, metabolism, and ABC transporters were significantly affected in both the *yfiQ* and *cobB* deletion mutants, indicating that protein acetylation not only controls prokaryotic chemotaxis, mobility, and energy metabolism, by direct acetylation of proteins or enzymes (4, 8, 15), but also regulates broad physiological functions in bacteria, by indirect activation and deactivation of gene expression. Surprisingly, the *cobB* and *yfiQ* gene deletions had similar impacts on the transcriptome profile of *Y. pestis*, which possibly resulted from the imbalance of acetylation and deacetylation in the *cobB* and *yfiQ* mutants. For instance, the virulence-related genes *hmsHFRS* and *psaABCDEF* were downregulated significantly in both mutants (Table 3), and the mouse infection experiments further confirmed the virulence attenuation of the Δ*cobB* and Δ*yfiQ* strains. Interestingly, we found that genes encoding heat shock

proteins (*htpG*, *hslV*, *hslR*, and *ibpA*), a cold shock protein (*cspA1*), acid resistance proteins (*hdeB* and *adiA*), and the regulator protein SlyA were also expressed at significantly lower levels in the Δ*cobB* or Δ*yfiQ* strain than in the wild-type bacterium. The phenotype analysis results showed that the *cobB* and *yfiQ* mutants had great impairments in their stress responses to heat and cold shock or to acidic pH and high-salt stimuli. These phenotype results are highly consistent with the findings of the comparative transcriptome analysis in this study. However, the mechanism underlying the virulence attenuation and lower tolerance of adverse environments of the *Y. pestis cobB* and *yfiQ* mutants needs further investigation.

MATERIALS AND METHODS

Bacterial strains and cell culture. *Y. pestis* bv. Microtus strain 201, which is avirulent to humans but highly virulent to mice, was used in this study (27). The bacterial strains and plasmids used are listed in Table 2. HeLa cells were maintained in Dulbecco's modified Eagle's medium (DMEM; HyClone, Little Chalfont, United Kingdom) containing 10% fetal bovine serum and 2 mM L-glutamine at 37°C in a 5% CO_2 incubator.

Construction of *cobB* and *yfiQ* mutants and complemented strains. The coding sequences of *cobB* and *yfiQ* were replaced by a kanamycin resistance cassette via the λ Red recombination system, and the pKD46 helper plasmid was eliminated at 43°C. The kanamycin resistance gene was eliminated by the FLP recombinase expressed by the pCP20 helper plasmid, which was itself then cured by growth at 43°C (28). Thus, we generated two null mutants (*cobB* and *yfiQ*) from *Y. pestis* strain 201.

To construct the complemented strains, a PCR-generated DNA fragment containing the *cobB* or *yfiQ* coding sequence together with ~300 bp of the respective upstream sequence was cloned into pACYC184. After DNA sequence verification, the recombinant plasmids expressing YfiQ and CobB were introduced into the Δ*cobB* and Δ*yfiQ* strains, respectively, yielding the complemented mutant strains, Com-*cobB* and Com-*yfiQ*.

Reagents and antibodies. NAD^+ and NAM were purchased from Sigma-Aldrich (St. Louis, MO, USA). IRDye 800CW-conjugated goat anti-rabbit antibody was purchased from Li-Cor Biosciences (Lincoln, NE, USA). Anti-His antibody and an anti-acetyl-lysine (Ac-K2-100) rabbit monoclonal antibody were purchased from Cell Signaling Technology (Danvers, MA, USA). Pierce bicinchoninic acid (BCA) protein assay kits were purchased from Thermo Fisher Scientific (Waltham, MA, USA). Amicon Ultra-15 regenerated cellulose centrifugal filter devices (3,000-Da molecular size cutoff) and Immobilon-P transfer membranes were purchased from Millipore (Bedford, MA, USA). Rabbit antibodies specific for CobB and YfiQ were prepared in our laboratory as described previously (29).

Bacterial growth curves. The *Y. pestis* strains were grown in LB broth or TMH medium (23) at 26°C to an OD_{620} of 1.0. Bacterial cultures were diluted 1:20 in fresh LB broth or TMH medium and then incubated at 26°C with shaking at 230 rpm, and the bacterial growth was monitored by measuring the OD_{620} (30). The experiments were performed on three independent cultures, and the results are expressed as means ± standard deviations (SD).

***cobB* and *yfiQ* gene expression in wild-type *Y. pestis* during different growth phases.** Overnight cultures in LB broth, each at an OD_{620} of about 1.0, were diluted 1:20 into 18 ml of fresh LB broth. The cultures were incubated at 26°C with shaking at 230 rpm to reach the early exponential phase (OD_{620} ≈ 0.5), mid-log phase (OD_{620} ≈ 1.0), and stationary phase (OD_{620} ≈ 1.5). Immediately before bacterial harvest for RNA isolation, a double volume of RNAprotect reagent (Qiagen, Valencia, CA) was mixed with the samples, and total RNA was extracted using TRIzol reagent (Invitrogen, Carlsbad, CA). *cobB* and *yfiQ* gene expression was examined by qRT-PCR, using the primers listed in Table S1 in the supplemental material and a Roche LightCycler 480 machine, as described previously (26).

Comparative transcriptome analysis of the wild-type strain and the mutants. The *cobB* and *yfiQ* mutants and the wild-type strain were individually inoculated into fresh TMH medium from the overnight cultures and grown at 26°C to the mid-log phase (OD_{620} ≈ 1.2). The bacterial cultures were pelleted, and total RNA was extracted using an Ambion PureLink RNA minikit (Invitrogen) according to the manufacturer's instructions. The isolated RNA samples were submitted to the Novogene Bioinformatics Technology Co., Ltd. (Beijing, China), for library construction and RNA sequencing. We used the numbers of fragments per kilobase of gene per million fragments mapped (FPKM) to calculate the gene expression levels (31). Clean reads from the different strains were mapped to the reference genome by using Bowtie 2 (version 2.2.3) (32). HTSeq v0.6.1 was used to count the read numbers mapped to each gene, the FPKM value of each gene was calculated based on the length of the gene, and read counts were mapped to the gene. Differential expression analysis of two groups (Δ*cobB*/wild type and Δ*yfiQ*/wild type; two biological replicates per strain) was performed using the R DESeq package (1.18.0). The resulting *P* values were adjusted using Benjamini and Hochberg's approach for controlling the false-discovery rate. An adjusted *P* value of <0.05 by DESeq and a $|\log_2$ fold change (Δ*cobB*/wild type or Δ*yfiQ*/wild type)| value of ≥ 1 were the thresholds set for DEG determination.

Functional analysis of DEGs was performed using DAVID bioinformatics tools (25) and according to the Kyoto Encyclopedia of Genes and Genomes (http://www.genome.jp/kegg/) and Gene Ontology (GO) annotations. The significance of KEGG pathways or GO term enrichment in DEGs was tested by Fisher's exact test followed by the Benjamini multiple-testing correction.

To verify the DEGs identified by the RNA-seq analysis, the expression of 19 genes (Tables S1 and S2) was determined by SYBR green I fluorescence-based qRT-PCR using a Roche LightCycler 480 machine

(Roche, Germany). The data were normalized to 16S rRNA gene expression in *Y. pestis*. Correlations between the qRT-PCR and RNA-seq data were analyzed by the linear regression method.

Protein expression and purification and antibody preparation. The *cobB* and *yfiQ* gene coding sequences were inserted into the pET28a and pGEX-4T-2 vectors, respectively. His-tagged PhoP and CobB of *Y. pestis* were expressed in *E. coli* BL21(DE3) by induction with 1 mM isopropyl-β-D-thiogalactopyranoside when the OD_{620} of the cultures reached about 0.6, followed by incubation overnight at 26°C. His-tagged proteins were purified by affinity chromatography with Ni-nitrilotriacetic acid (Ni-NTA) agarose, and the glutathione *S*-transferase (GST)–YfiQ protein was purified by use of glutathione Sepharose 4B beads as described previously (33). The buffers containing the purified proteins were exchanged for phosphate-buffered saline by use of PD-10 desalting columns (GE Healthcare, Pittsburgh, PA, USA). The purified CobB and YfiQ proteins were used as immunogens to provoke the production of polyclonal antibodies in rabbits, and IgGs specific for CobB or YfiQ were purified as described previously (34).

***In vitro* acetylation and deacetylation assays.** Concentrations of the purified PhoP, YfiQ, and CobB proteins were determined by use of a Pierce BCA protein assay kit. For the acetylation assay, 20 μg of PhoP was incubated with 10 μg of YfiQ in 100 μl of buffer containing 50 mM Tris-HCl (pH 8.0), 0.1 mM EDTA, 10% glycerol, 1 mM dithiothreitol, 10 mM sodium butyrate, and 0.2 mM Ac-CoA. The reaction mixtures were mixed thoroughly and incubated at 37°C for 6 h. For the deacetylation assay, 10 μg of PhoP was incubated with 5 μg of CobB in deacetylation reaction buffer containing 50 mM Tris-HCl (pH 8.0), 135 mM NaCl, 2.5 mM KCl, and 1 mM $MgCl_2$ in the presence or absence of 4 mM NAD^+ and 40 mM NAM. After incubation, the acetylation status of PhoP was analyzed by SDS-PAGE and immunoblotting using anti-His and anti-acetyl-lysine (Ac-K2-100) rabbit monoclonal antibodies (22). Images of the immunoblotting results were acquired with an Odyssey SA imaging system (Li-Cor). Protein band intensities were quantitated using ImageJ 1.50i software (http://rsbweb.nih.gov/ij/).

Virulence determination. The Δ*cobB*, Δ*yfiQ*, and wild-type *Y. pestis* strains were grown separately in LB medium at 26°C. For each strain tested, 10 female BALB/c mice (6 to 8 weeks old) were injected subcutaneously with 100 CFU of the bacterial strain, and the infected animals were observed daily for 14 days. The survival rate for each animal group was calculated, and statistical significance was calculated by the log rank (Mantel-Cox) test, using GraphPad Prism 5 software. All animal experiments were carried out in accordance with the guidelines for the welfare and ethics of laboratory animals of China and approved by the Committee of Laboratory Animal Welfare and Ethics of the Institute for Endemic Disease Prevention and Control of Qinghai Province, China (approval no. 20151004).

Stress response assays. (i) Acid resistance. *Y. pestis* strains were grown in TMH medium at 26°C to an OD_{620} of ≈1.0. The bacterial cells were harvested, washed twice with phosphate-buffered saline, and resuspended in *Y. pestis* minimal medium (MM) supplemented with a 1 mM concentration of the essential amino acid for *Y. pestis* strain 201 (L-arginine) and 20 mM glucose as a carbon source (35). A 1:100 dilution of the resuspended bacterial cells was added to MM, pH 3.5, or MM, pH 7.0, to serve as a control. After 30 or 60 min, the bacterial suspensions were diluted and plated on Hottinger's agar to determine the number of viable bacteria (36). All the samples were analyzed in triplicate, and the bacterial survival rate was calculated by dividing the number of viable cells in the stress condition-treated samples by that for the controls. Two-way analysis of variance (ANOVA) with Bonferroni's multiple-comparison test was performed using GraphPad Prism 5 software to analyze the significance of the differences between the various strains.

(ii) Heat and cold resistance. Bacterial strains were cultivated, collected, and resuspended as described for the acid resistance assay. Bacterial suspensions were transferred to 50°C for 10 min or 20 min for the heat shock treatment or to 0°C, 4°C, or 20°C for 24 h for cold shock treatment (37). A bacterial suspension incubated at 26°C served as the untreated control. The survival rates were calculated and statistically analyzed as described in the acid resistance section.

(iii) High-salt resistance. *Y. pestis* strains were grown in LB medium at 26°C to an OD_{620} of ≈1.0. The bacterial cultures were diluted 1:20 in LB medium containing 4% NaCl and incubated at 26°C with shaking at 230 rpm. Bacterial growth was monitored by measuring the OD_{620}. The experiments were performed twice independently, and results representative of one experiment are shown.

Biofilm assays. Bacterial biofilm formation ability was analyzed using the crystal violet staining method as described previously (38). *Y. pestis* strains were inoculated into 24-well tissue culture plates with 1 ml of culture in each well and then incubated at 26°C for 24 h. The culture medium containing the planktonic cells was removed from each well to determine the OD_{620}. Wells with adherent biofilms were washed gently three times with 2 ml of H_2O and then fixed at 80°C for 15 min. The surface-attached cells were stained with 3 ml of 0.1% crystal violet for 15 min. The solution was removed, the wells were washed three times with 3 ml of H_2O, and the pigment in the wells was dissolved with 3 ml of dimethyl sulfoxide. The OD_{570} values were recorded and the OD_{570}/OD_{620} calculated. The experiments were performed using three independent bacterial cultures, and the values shown are means ± standard deviations. Statistical analysis was performed as described in the acid resistance section.

SUPPLEMENTAL MATERIAL

Supplemental material for this article may be found at https://doi.org/10.1128/IAI.00224-18.

SUPPLEMENTAL FILE 1, PDF file, 1.1 MB.

ACKNOWLEDGMENTS

This work was supported by the National Natural Science Foundation of China (grant 31470242), the Special Key Project of Biosafety Technologies for the National Major Research and Development Program of China (grant 2017YFC1200800), and the Basic Research Programs of Science and Technology Department Foundation of Qinghai Province (grant 2013-Z-748).

We thank Shimin Zhao (Fudan University, Shaihai, China), Qijun Wang (Fudan University, Shaihai, China), and Yufeng Yao (Shanghai Jiao Tong University, Shanghai, China) for their generous gift of the anti-acetyl-lysine antibody and for helpful discussions. We thank Sandra Cheesman, from Liwen Bianji, Edanz Group China, for editing the English text of a draft of the manuscript.

REFERENCES

1. Hu LI, Lima BP, Wolfe AJ. 2010. Bacterial protein acetylation: the dawning of a new age. Mol Microbiol 77:15–21. https://doi.org/10.1111/j.1365-2958.2010.07204.x.
2. Allfrey VG, Faulkner R, Mirsky AE. 1964. Acetylation and methylation of histones and their possible role in the regulation of RNA synthesis. Proc Natl Acad Sci U S A 51:786–794.
3. Yu BJ, Kim JA, Moon JH, Ryu SE, Pan JG. 2008. The diversity of lysine-acetylated proteins in Escherichia coli. J Microbiol Biotechnol 18:1529–1536.
4. Wang Q, Zhang Y, Yang C, Xiong H, Lin Y, Yao J, Li H, Xie L, Zhao W, Yao Y, Ning ZB, Zeng R, Xiong Y, Guan KL, Zhao S, Zhao GP. 2010. Acetylation of metabolic enzymes coordinates carbon source utilization and metabolic flux. Science 327:1004–1007. https://doi.org/10.1126/science.1179687.
5. Kim D, Yu BJ, Kim JA, Lee YJ, Choi SG, Kang S, Pan JG. 2013. The acetylproteome of Gram-positive model bacterium Bacillus subtilis. Proteomics 13:1726–1736. https://doi.org/10.1002/pmic.201200001.
6. Zhang K, Zheng S, Yang JS, Chen Y, Cheng Z. 2013. Comprehensive profiling of protein lysine acetylation in Escherichia coli. J Proteome Res 12:844–851. https://doi.org/10.1021/pr300912q.
7. Liu F, Yang M, Wang X, Yang S, Gu J, Zhou J, Zhang XE, Deng J, Ge F. 2014. Acetylome analysis reveals diverse functions of lysine acetylation in Mycobacterium tuberculosis. Mol Cell Proteomics 13:3352–3366. https://doi.org/10.1074/mcp.M114.041962.
8. Castano-Cerezo S, Bernal V, Post H, Fuhrer T, Cappadona S, Sanchez-Diaz NC, Sauer U, Heck AJ, Altelaar AF, Canovas M. 2014. Protein acetylation affects acetate metabolism, motility and acid stress response in Escherichia coli. Mol Syst Biol 10:762. https://doi.org/10.15252/msb.20145227.
9. Wolfe AJ. 2016. Bacterial protein acetylation: new discoveries unanswered questions. Curr Genet 62:335–341. https://doi.org/10.1007/s00294-015-0552-4.
10. Nambi S, Basu N, Visweswariah SS. 2010. cAMP-regulated protein lysine acetylases in mycobacteria. J Biol Chem 285:24313–24323. https://doi.org/10.1074/jbc.M110.118398.
11. Starai VJ, Escalante-Semerena JC. 2004. Identification of the protein acetyltransferase (Pat) enzyme that acetylates acetyl-CoA synthetase in Salmonella enterica. J Mol Biol 340:1005–1012. https://doi.org/10.1016/j.jmb.2004.05.010.
12. Starai VJ, Celic I, Cole RN, Boeke JD, Escalante-Semerena JC. 2002. Sir2-dependent activation of acetyl-CoA synthetase by deacetylation of active lysine. Science 298:2390–2392. https://doi.org/10.1126/science.1077650.
13. Hu LI, Chi BK, Kuhn ML, Filippova EV, Walker-Peddakotla AJ, Basell K, Becher D, Anderson WF, Antelmann H, Wolfe AJ. 2013. Acetylation of the response regulator RcsB controls transcription from a small RNA promoter. J Bacteriol 195:4174–4186. https://doi.org/10.1128/JB.00383-13.
14. Castano-Cerezo S, Bernal V, Blanco-Catala J, Iborra JL, Canovas M. 2011. cAMP-CRP co-ordinates the expression of the protein acetylation pathway with central metabolism in Escherichia coli. Mol Microbiol 82:1110–1128. https://doi.org/10.1111/j.1365-2958.2011.07873.x.
15. Li R, Gu J, Chen YY, Xiao CL, Wang LW, Zhang ZP, Bi LJ, Wei HP, Wang XD, Deng JY, Zhang XE. 2010. CobB regulates Escherichia coli chemotaxis by deacetylating the response regulator CheY. Mol Microbiol 76:1162–1174. https://doi.org/10.1111/j.1365-2958.2010.07125.x.
16. Lima BP, Thanh Huyen TT, Basell K, Becher D, Antelmann H, Wolfe AJ. 2012. Inhibition of acetyl phosphate-dependent transcription by an acetylatable lysine on RNA polymerase. J Biol Chem 287:32147–32160. https://doi.org/10.1074/jbc.M112.365502.
17. Thao S, Chen CS, Zhu H, Escalante-Semerena JC. 2010. Nepsilon-lysine acetylation of a bacterial transcription factor inhibits its DNA-binding activity. PLoS One 5:e15123. https://doi.org/10.1371/journal.pone.0015123.
18. Bernal V, Castano-Cerezo S, Gallego-Jara J, Ecija-Conesa A, de Diego T, Iborra JL, Canovas M. 2014. Regulation of bacterial physiology by lysine acetylation of proteins. New Biotechnol 31:586–595. https://doi.org/10.1016/j.nbt.2014.03.002.
19. Zhang QF, Gu J, Gong P, Wang XD, Tu S, Bi LJ, Yu ZN, Zhang ZP, Cui ZQ, Wei HP, Tao SC, Zhang XE, Deng JY. 2013. Reversibly acetylated lysine residues play important roles in the enzymatic activity of Escherichia coli N-hydroxyarylamine O-acetyltransferase. FEBS J 280:1966–1979. https://doi.org/10.1111/febs.12216.
20. Parkhill J, Wren BW, Thomson NR, Titball RW, Holden MT, Prentice MB, Sebaihia M, James KD, Churcher C, Mungall KL, Baker S, Basham D, Bentley SD, Brooks K, Cerdeno-Tarraga AM, Chillingworth T, Cronin A, Davies RM, Davis P, Dougan G, Feltwell T, Hamlin N, Holroyd S, Jagels K, Karlyshev AV, Leather S, Moule S, Oyston PC, Quail M, Rutherford K, Simmonds M, Skelton J, Stevens K, Whitehead S, Barrell BG. 2001. Genome sequence of Yersinia pestis, the causative agent of plague. Nature 413:523–527. https://doi.org/10.1038/35097083.
21. Song Y, Tong Z, Wang J, Wang L, Guo Z, Han Y, Zhang J, Pei D, Zhou D, Qin H, Pang X, Zhai J, Li M, Cui B, Qi Z, Jin L, Dai R, Chen F, Li S, Ye C, Du Z, Lin W, Yu J, Yang H, Huang P, Yang R. 2004. Complete genome sequence of *Yersinia pestis* strain 91001, an isolate avirulent to humans. DNA Res 11:179–197. https://doi.org/10.1093/dnares/11.3.179.
22. Ren J, Sang Y, Tan Y, Tao J, Ni J, Liu S, Fan X, Zhao W, Lu J, Wu W, Yao YF. 2016. Acetylation of lysine 201 inhibits the DNA-binding ability of PhoP to regulate Salmonella virulence. PLoS Pathog 12:e1005458. https://doi.org/10.1371/journal.ppat.1005458.
23. Straley SC, Bowmer WS. 1986. Virulence genes regulated at the transcriptional level by Ca^{2+} in Yersinia pestis include structural genes for outer membrane proteins. Infect Immun 51:445–454.
24. Anders S, Huber W. 2010. Differential expression analysis for sequence count data. Genome Biol 11:R106. https://doi.org/10.1186/gb-2010-11-10-r106.
25. Huang DW, Sherman BT, Lempicki RA. 2009. Systematic and integrative analysis of large gene lists using DAVID bioinformatics resources. Nat Protoc 4:44–57. https://doi.org/10.1038/nprot.2008.211.
26. Liu L, Fang H, Yang H, Zhang Y, Han Y, Zhou D, Yang R. 2016. Reciprocal regulation of Yersinia pestis biofilm formation and virulence by RovM and RovA. Open Biol 6:150198. https://doi.org/10.1098/rsob.150198.
27. Zhou D, Tong Z, Song Y, Han Y, Pei D, Pang X, Zhai J, Li M, Cui B, Qi Z, Jin L, Dai R, Du Z, Wang J, Guo Z, Wang J, Huang P, Yang R. 2004. Genetics of metabolic variations between Yersinia pestis biovars and the proposal of a new biovar, microtus. J Bacteriol 186:5147–5152. https://doi.org/10.1128/JB.186.15.5147-5152.2004.
28. Datsenko KA, Wanner BL. 2000. One-step inactivation of chromosomal genes in Escherichia coli K-12 using PCR products. Proc Natl Acad Sci U S A 97:6640–6645. https://doi.org/10.1073/pnas.120163297.
29. Yang H, Tan Y, Zhang T, Tang L, Wang J, Ke Y, Guo Z, Yang X, Yang R, Du Z. 2013. Identification of novel protein-protein interactions of *Yersinia*

pestis type III secretion system by yeast two hybrid system. PLoS One 8:e54121. https://doi.org/10.1371/journal.pone.0054121.
30. Deng Z, Liu Z, He J, Wang J, Yan Y, Wang X, Cui Y, Bi Y, Du Z, Song Y, Yang R, Han Y. 2015. TyrR, the regulator of aromatic amino acid metabolism, is required for mice infection of Yersinia pestis. Front Microbiol 6:110. https://doi.org/10.3389/fmicb.2015.00110.
31. Medzhitov R, Janeway C, Jr. 2000. Innate immune recognition: mechanisms and pathways. Immunol Rev 173:89–97. https://doi.org/10.1034/j.1600-065X.2000.917309.x.
32. Langmead B, Trapnell C, Pop M, Salzberg SL. 2009. Ultrafast and memory-efficient alignment of short DNA sequences to the human genome. Genome Biol 10:R25. https://doi.org/10.1186/gb-2009-10-3-r25.
33. Cao SY, Liu WB, Tan YF, Yang HY, Zhang TT, Wang T, Wang XY, Song YJ, Yang RF, Du ZM. 2017. An interaction between the inner rod protein YscI and the needle protein YscF is required to assemble the needle structure of the Yersinia type three secretion system. J Biol Chem 292:5488–5498. https://doi.org/10.1074/jbc.M116.743591.
34. Yang F, Ke Y, Tan Y, Bi Y, Shi Q, Yang H, Qiu J, Wang X, Guo Z, Ling H, Yang R, Du Z. 2010. Cell membrane is impaired, accompanied by enhanced type III secretion system expression in Yersinia pestis deficient in RovA regulator. PLoS One 5:e12840. https://doi.org/10.1371/journal.pone.0012840.
35. Sebbane F, Jarrett CO, Linkenhoker JR, Hinnebusch BJ. 2004. Evaluation of the role of constitutive isocitrate lyase activity in Yersinia pestis infection of the flea vector and mammalian host. Infect Immun 72:7334–7337. https://doi.org/10.1128/IAI.72.12.7334-7337.2004.
36. Hommais F, Krin E, Laurent-Winter C, Soutourina O, Malpertuy A, Le Caer JP, Danchin A, Bertin P. 2001. Large-scale monitoring of pleiotropic regulation of gene expression by the prokaryotic nucleoid-associated protein, H-NS. Mol Microbiol 40:20–36. https://doi.org/10.1046/j.1365-2958.2001.02358.x.
37. Li DC, Yang F, Lu B, Chen DF, Yang WJ. 2012. Thermotolerance and molecular chaperone function of the small heat shock protein HSP20 from hyperthermophilic archaeon, Sulfolobus solfataricus P2. Cell Stress Chaperones 17:103–108. https://doi.org/10.1007/s12192-011-0289-z.
38. Sun F, Gao H, Zhang Y, Wang L, Fang N, Tan Y, Guo Z, Xia P, Zhou D, Yang R. 2012. Fur is a repressor of biofilm formation in Yersinia pestis. PLoS One 7:e52392. https://doi.org/10.1371/journal.pone.0052392.
39. Han Y, Zhou D, Pang X, Song Y, Zhang L, Bao J, Tong Z, Wang J, Guo Z, Zhai J, Du Z, Wang X, Zhang X, Wang J, Huang P, Yang R. 2004. Microarray analysis of temperature-induced transcriptome of Yersinia pestis. Microbiol Immunol 48:791–805. https://doi.org/10.1111/j.1348-0421.2004.tb03605.x.